Developmental Cell
Article

The BH3-Only SNARE BNip1 Mediates Photoreceptor Apoptosis in Response to Vesicular Fusion Defects

Yuko Nishiwaki,[1] Asuka Yoshizawa,[1] Yutaka Kojima,[1] Eri Oguri,[1] Shohei Nakamura,[1] Shohei Suzuki,[1] Junichi Yuasa-Kawada,[1] Mariko Kinoshita-Kawada,[1] Toshiaki Mochizuki,[1] and Ichiro Masai[1,*]
[1]Developmental Neurobiology Unit, Okinawa Institute of Science and Technology Graduate University, 1919-1 Tancha, Onna, Okinawa 904-0412, Japan
*Correspondence: masai@oist.jp
http://dx.doi.org/10.1016/j.devcel.2013.04.015

SUMMARY

Intracellular vesicular transport is important for photoreceptor function and maintenance. However, the mechanism underlying photoreceptor degeneration in response to vesicular transport defects is unknown. Here, we report that photoreceptors undergo apoptosis in a zebrafish β-soluble N-ethylmaleimide-sensitive factor attachment protein (β-SNAP) mutant. β-SNAP cooperates with N-ethylmaleimide-sensitive factor to recycle the SNAP receptor (SNARE), a key component of the membrane fusion machinery, by disassembling the *cis*-SNARE complex generated in the vesicular fusion process. We found that photoreceptor apoptosis in the β-SNAP mutant was dependent on the BH3-only protein BNip1. BNip1 functions as a component of the syntaxin-18 SNARE complex and regulates retrograde transport from the Golgi to the endoplasmic reticulum. Failure to disassemble the syntaxin-18 *cis*-SNARE complex caused BNip1-dependent apoptosis. These data suggest that the syntaxin-18 *cis*-SNARE complex functions as an alarm factor that monitors vesicular fusion competence and that BNip1 transforms vesicular fusion defects into photoreceptor apoptosis.

INTRODUCTION

More than a hundred genes associated with inherited photoreceptor degeneration have been identified in humans (Kennan et al., 2005; Pacione et al., 2003). The importance of protein transport in photoreceptor maintenance has been suggested by studies involving genetic mutations of the visual pigment rhodopsin, which compromise its transport to photoreceptive membranes along the secretory pathway (Deretic et al., 1998; Mendes et al., 2005; Sung et al., 1991; Tam and Moritz, 2007), and regulatory factors involved in intraflagellar transport through the connecting cilium (Eley et al., 2005). However, the mechanism underlying the link between defects in protein transport and photoreceptor degeneration remains to be elucidated.

Protein transport between membrane compartments along the secretory pathway is primarily mediated by vesicles that bud from donor compartments followed by targeting to, docking onto, and fusion with acceptor membranes (Bonifacino and Glick, 2004; Rothman, 1994). Three key factors, namely, N-ethylmaleimide-sensitive factor (NSF) (Wilson et al., 1989), soluble NSF attachment protein (SNAP) (Clary et al., 1990), and SNAP receptor (SNARE) (Söllner et al., 1993), are involved in the fusion process. SNARE proteins form a superfamily and are classified into two groups: vesicle-membrane SNAREs (v-SNAREs) and target-membrane SNAREs (t-SNAREs) (Jahn and Scheller, 2006). Three t-SNAREs form the acceptor SNARE complex on target membranes and subsequently interact with one v-SNARE to trigger the docking and fusion process. The acceptor SNARE complex and v-SNARE pair to form a *cis*-SNARE complex on fused membranes. SNAP then binds to the *cis*-SNARE complex and recruits NSF. NSF is a member of the AAA (ATPase associated with diverse cellular activity) protein family, and ATP hydrolysis by NSF disassembles the *cis*-SNARE complex for the recycling of SNAREs. Combinatorial pairing between v-SNAREs and t-SNAREs is thought to ensure compartmental specificity of membrane fusion (McNew et al., 2000), but both NSF and SNAP seem to function on all *cis*-SNARE complexes.

Three mammalian forms of SNAPs have been identified, and these are referred to as α-SNAP, β-SNAP, and γ-SNAP (Clary et al., 1990). β-SNAP is brain specific and highly homologous to α-SNAP (Whiteheart et al., 1993), whereas α-SNAP and γ-SNAP are widely distributed and exhibit 25% amino acid identity. In eukaryotes, α-SNAP is involved in diverse types of membrane fusion events, such as anterograde transport from the endoplasmic reticulum (ER) to the Golgi (Kaiser and Schekman, 1990; Peter et al., 1998), intracompartmental transport in the Golgi complex (Clary and Rothman, 1990), and synaptic vesicle exocytosis for neurotransmitter release (Babcock et al., 2004; Burgalossi et al., 2010). β-SNAP has been reported to cooperate with α-SNAP to promote the recycling of synaptic SNAREs (Burgalossi et al., 2010). However, the biological roles of β-SNAP are not fully understood.

BNip1 was shown to be a protein that is capable of interacting with the antiapoptotic adenovirus E1B 19 kDa protein (Boyd et al., 1994). BNip1 has a Bcl2 homology domain 3 (BH3), and its overexpression results in moderate proapoptotic activity (Nakajima et al., 2004; Yasuda and Chinnadurai, 2000). BNip1 also functions as a t-SNARE and a component of the syntaxin-18 complex,

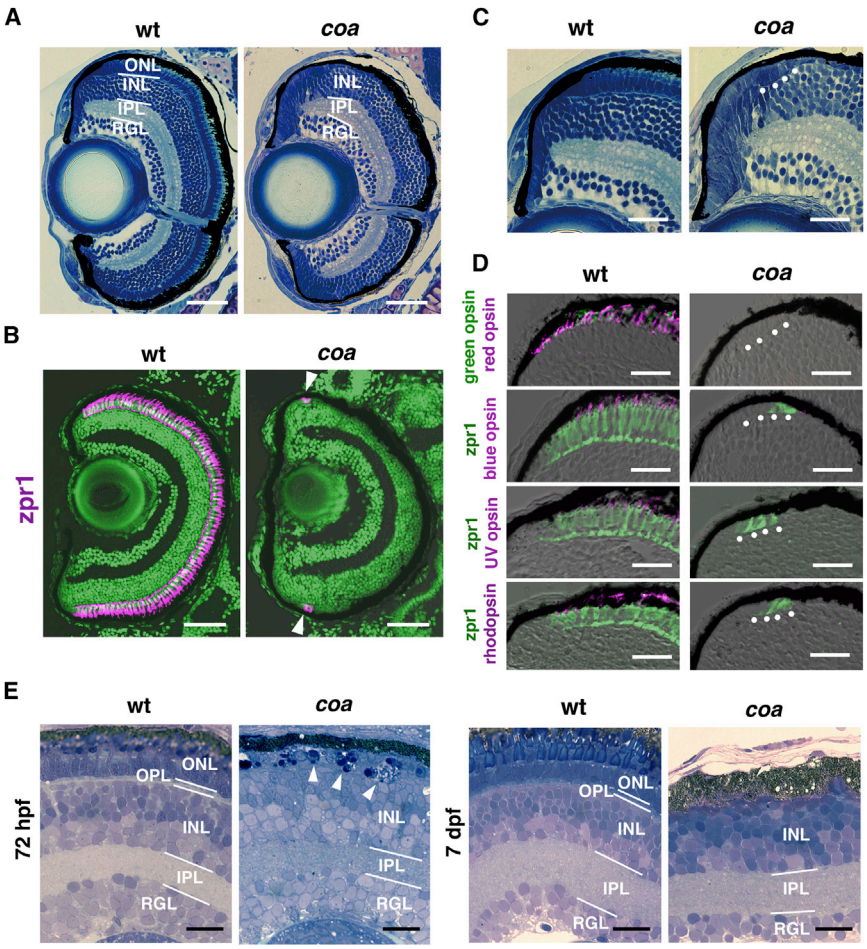

Figure 1. Photoreceptors Undergo Apoptosis in the Zebrafish *coa* Mutant

(A) Plastic sections of WT and *coa* mutant retinas at 6 dpf. ONL is absent in the *coa* mutant.

(B) Zpr1 antibody labeling of 6 dpf WT and *coa* mutant retinas. All nuclei are counterstained with SYTOX Green (green). Arrowheads indicate zpr1 expression (magenta) in the CMZ of the *coa* mutant.

(C) Plastic sections of CMZ of 6 dpf WT and *coa* mutant retinas. White dots indicate morphologically distinct ONL in the *coa* mutant.

(D) Labeling of 6 dpf WT and *coa* mutant retinas with anti-red, blue, UV opsins, or rhodopsin antibodies (magenta); anti-green opsin antibody (green); and zpr1 (green) antibody.

(E) Semithin sections of WT and *coa* mutant retinas at 72 hpf and 7 dpf. At 72 hpf, pyknotic nuclei were observed in the ONL in the *coa* mutant (arrowheads). At 7 dpf, ONL was absent in the *coa* mutant.

INL, inner nuclear layer; IPL, inner plexiform layer; OPL, outer plexiform layer; RGL, retinal ganglion cell layer. Scale bars, 50 μm (A and B) and 20 μm (C–E). See also Figure S1.

which regulates retrograde vesicular transport from the Golgi to the ER (Nakajima et al., 2004). The syntaxin-18 complex contains three t-SNARE components, namely, syntaxin-18 (Hatsuzawa et al., 2000), BNip1, and unconventional SNARE in the ER1 (Use1) (Hirose et al., 2004), and a v-SNARE, namely, Sec22b (Aoki et al., 2008). A previous study using human cell cultures showed that overexpression of α-SNAP inhibited the proapoptotic activity of BNip1 (Nakajima et al., 2004). However, the biological significance of α-SNAP-mediated suppression of BNip1 proapoptotic activity remains to be elucidated.

In this study, we found that photoreceptors underwent apoptosis prior to maturation in the zebrafish β-SNAP mutant, suggesting that vesicular fusion defects induce photoreceptor apoptosis. Photoreceptor apoptosis in zebrafish β-SNAP mutants was dependent on BNip1. Failed disassembly of the syntaxin-18 *cis*-SNARE complex activates BNip1-dependent apoptosis. These data suggest that β-SNAP normally suppresses BNip1 proapoptotic activity by disassembling the syntaxin-18 *cis*-SNARE complex. Because available β-SNAP represents vesicular fusion competence, the syntaxin-18 *cis*-SNARE complex functions as an alarm factor that senses vesicular fusion competence, and BNip1 transforms vesicular fusion defects into photoreceptor apoptosis. Our findings indicate a role for BNip1 in linking vesicular fusion competence and photoreceptor apoptosis.

RESULTS

Photoreceptors Degenerate in the Zebrafish *coa* Mutant

In a previous work (Nishiwaki et al., 2008), we isolated the zebrafish *corona* (*coa*) mutant, which exhibits photoreceptor degeneration. In wild-type (WT) zebrafish, all retinal cell types differentiate by 6 days postfertilization (dpf). However, the outer nuclear layer (ONL), which consists of photoreceptors, was exclusively absent in the *coa* mutant (Figure 1A). In WT fish, an early marker of double-cone photoreceptors, zpr1 (Larison and Bremiller, 1990), was expressed in the ONL at 6 dpf. However, zpr1 expression was only detected in the ciliary marginal zone (CMZ), a peripheral part of the retina, in the *coa* mutant (Figure 1B). Because retinal stem cells are located in the CMZ and generate retinal neurons, this transient zpr1 expression in the CMZ suggests that photoreceptors start to differentiate but degenerate during their maturation. Consistently, the ONL was morphologically distinct only near the CMZ in the *coa* mutant at 6 dpf (Figure 1C). Although these ONL cells expressed zpr1, protein expression of rhodopsin and opsins was markedly reduced (Figure 1D). Next, we examined the *coa* mutant retina during developmental stages. In the *coa* mutant, the ONL was formed at 60 hr postfertilization (hpf) in the central retina (data not shown), but photoreceptors underwent cell death at 72 hpf and the ONL was completely eliminated by 7 dpf (Figure 1E). Thus, retinal photoreceptors are initially specified but undergo degeneration prior to their maturation in the *coa* mutant.

Next, we carried out electron microscopy (EM) analyses. In WT photoreceptors at 54 hpf, multistacked membrane discs called the outer segment (OS) formed in the most apical region (Figure S1A available online), and tubular cisternae reminiscent of

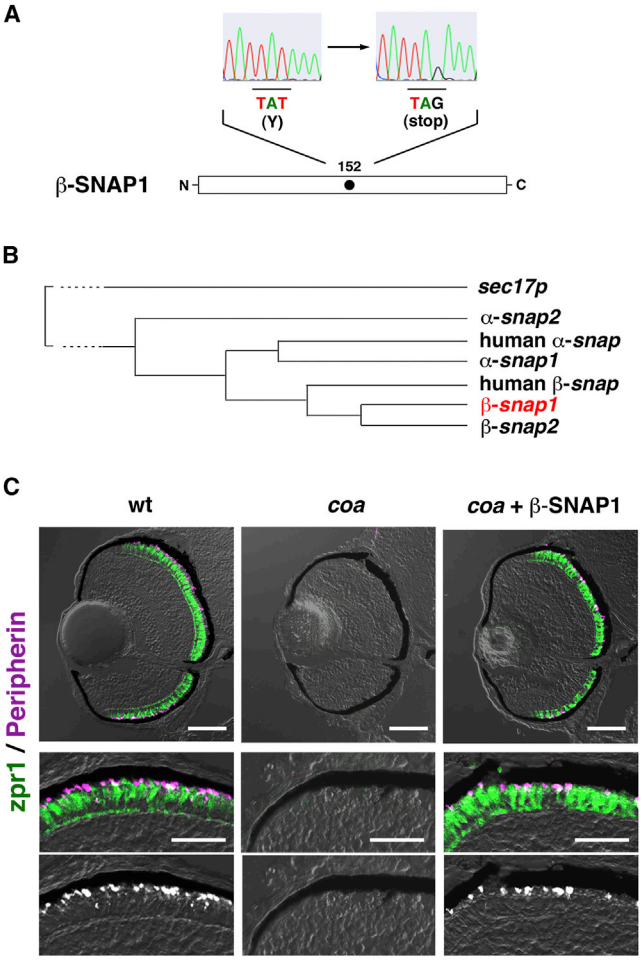

Figure 2. The *coa* Mutant Gene Encodes β-SNAP1

(A) A non-sense mutation occurs at 152Y in *β-snap1* gene in the *coa* mutant.

(B) There are four zebrafish *snap* genes: two *α-snap* and two *β-snap* genes. β-SNAP1 has 90.8% amino acid identity to β-SNAP2, whereas β-SNAP1 has 78% and 73% amino acid identity to α-SNAP1 and α-SNAP2, respectively. In accordance with the evolution tree, zebrafish *α-snap2* gene is positioned outside the human *α-snap* gene. Zebrafish *β-snap* genes seem to be duplicated after separation from human *β-snap* gene. *sec17p* is a yeast α-SNAP homologous gene.

(C) Labeling of 84 hpf WT, *coa* mutant retinas, and *coa* mutant retinas expressing β-SNAP1 with zpr1 antibody (green) and GFP-tagged peripherin (magenta). Middle panels show higher magnification of the outer photoreceptor layer. Lower panels show the magenta channel. Scale bars, 50 μm (upper panels) and 10 μm (middle panels).

See also Figure S2.

the Golgi apparatus developed between the nucleus and the mitochondria-rich region, which is called the ellipsoid (Figure S1B). However, in *coa* mutant photoreceptors, the OS was mostly absent (Figure S1C) and tubular cisternae were not fully developed (Figure S1D). At 72 hpf, these defects became more evident (Figures S1E–S1K) and abnormally shaped nuclei were also observed (Figure S1L). At 7 dpf, the ONL was completely absent in the *coa* mutant (Figure S1M). To visualize the ER and Golgi, we injected a mixture of RNAs encoding the ER-retention peptide sequence fused to monomeric Kusabira Orange (ER-mKO) and the N-terminal 100 amino acids of mannosidase fused to GFP (Golgi-GFP) (Insinna et al., 2010) into zebrafish eggs. In WT photoreceptors at 60–76 hpf, ER-mKO was observed in the region surrounding the nucleus, whereas Golgi-GFP was observed in the region apical of the nucleus (Figure S1N). In *coa* mutant photoreceptors, expression of both fusion proteins was normal at 60 hpf. However, although ER-mKO was detected, Golgi-GFP became faint in the *coa* mutant photoreceptors at 72–76 hpf (Figure S1N). These data suggest that the Golgi was reduced in amount or dispersed in the *coa* mutant at the initial stage of degeneration. These observations suggest that the maintenance of intracellular membrane organelles such as the Golgi apparatus and the OS are compromised in the *coa* mutant.

The *coa* Mutant Gene Encodes β-SNAP

To elucidate whether the *coa* mutation behaves in a cell-autonomous manner, we carried out cell transplantation. When WT donor cells were incorporated into the *coa* mutant recipient retina, WT cells survived to express zpr1 and rhodopsin, suggesting that the *coa* mutant gene is required for photoreceptor maintenance cell autonomously (Figure S2A). Next, we mapped the *coa* mutation on zebrafish chromosomes using polymorphic markers. The *coa* mutation was mapped to chromosome 20. A polymorphic marker associated with the *β-snap* gene showed no recombination in 1,120 meioses (see Supplemental Experimental Procedures; Figure S2B). Furthermore, a non-sense mutation occurred at the codon encoding Tyr-152 in the *β-snap* gene in the *coa* mutant (Figure 2A). These data suggest that the *coa* mutant gene encodes β-SNAP. In the zebrafish genomic database, two *α-snap* genes and another *β-snap* gene mapped to chromosomes 5, 18, and 17, respectively. In this study, we designated the *coa* mutant gene as *β-snap1*, another *β-snap* gene as *β-snap2*, and two *α-snap* genes, which mapped to chromosomes 18 and 5, as *α-snap1* and *α-snap2*, respectively (Table S1; Figure 2B).

We examined whether overexpression of β-SNAP1 could rescue photoreceptor survival and protein transport to the OS in the *coa* mutant, using a zpr1 antibody to identify cone photoreceptors and a zebrafish transgenic line expressing GFP-tagged peripherin under the control of the *Xenopus rhodopsin* promoter to monitor protein transport in rod photoreceptors (Loewen et al., 2003). Peripherin is an integral membrane protein located at the OS membrane rim in photoreceptors, and its mutations are known to cause autosomal-dominant retinitis pigmentosa in humans (Kajiwara et al., 1993; Wells et al., 1993). In WT zebrafish, GFP-tagged peripherin was localized in the most apical region of rod photoreceptors, which corresponded to the OS (Figure 2C). In the *coa* mutant, GFP-tagged peripherin expression was not detected (Figure 2C). Overexpression of β-SNAP1 rescued not only photoreceptor survival but also the localization of GFP-tagged peripherin to the OS in the *coa* mutant (Figure 2C), confirming that the *coa* mutant gene encodes β-SNAP1. Next, we examined the redundancy of other SNAPs in the rescue of *coa* mutant defects. β-SNAP2 was as efficient as β-SNAP1 in rescuing the *coa* mutant defects, whereas α-SNAP1 and α-SNAP2 were less efficient (Figures S2C and S2D). Furthermore, the expression patterns of all four *snap* genes were similar by the 18 somite stage (Figure S2E). After 48 hpf, *β-snap1* messenger RNA (mRNA) was expressed

in the retina, including photoreceptors, whereas *β-snap2* mRNA expression was very low in the retina. Although β-SNAP2 functions similarly to β-SNAP1 in rescuing *coa* mutant defects, the more prominent expression of *β-snap1* in the retina after 48 hpf may explain photoreceptor degeneration in the *coa* mutant.

Photoreceptor Degeneration in the *coa* Mutant Is Dependent on BNip1

Mitochondria-dependent apoptosis is mediated by the activation of the proapoptotic Bcl2 family proteins Bak and Bax (Tait and Green, 2010; Westphal et al., 2011). The antiapoptotic Bcl2 family proteins Bcl2 and BclXL inhibit Bak/Bax-dependent apoptosis. Two *bax* genes, *bax1* and *bax2* (Kratz et al., 2006), and one *bcl2* gene (Langenau et al., 2005) are annotated in the zebrafish genomic database (Table S1). In contrast to the negative control *egfp* mRNA, overexpression of *bcl2* mRNA inhibited photoreceptor degeneration in the *coa* mutant (Figures 3A and 3B; Table S2). In zebrafish, *bax2* mRNA is expressed at the 1,000 cell stage, but its expression level becomes low in later stages, whereas *bax1* mRNA is constantly expressed from the 1,000 cell stage until 72 hpf (Kratz et al., 2006). We injected the *coa* mutant embryos with morpholinos against Bax1 (MO-Bax1) and Bax2 (MO-Bax2). Both MO-Bax1 and a mixture of MO-Bax1 and MO-Bax2 inhibited photoreceptor degeneration in the *coa* mutant, whereas MO-Bax2 alone did not (Figures 3C and 3D), suggesting that mitochondria-dependent apoptosis mediates photoreceptor degeneration in the *coa* mutant through Bax1.

BH3-only proteins modulate apoptosis by regulating the balance between antiapoptotic and proapoptotic Bcl2 family proteins (Lomonosova and Chinnadurai, 2008; Tait and Green, 2010). BNip1 is a BH3-only protein that interacts with Bcl2 (Boyd et al., 1994) and functions as a t-SNARE component of the syntaxin-18 complex, which regulates retrograde transport from the Golgi to the ER (Nakajima et al., 2004). A previous study suggested that overexpression of human α-SNAP suppresses BNip1 proapoptotic activity (Nakajima et al., 2004). Because human α-SNAP has 81% amino acid identity to zebrafish β-SNAP1, we examined the possibility that photoreceptor apoptosis in the *coa* mutant depends on BNip1. In the zebrafish database, two BNip1 homologous genes, namely, *bnip1a* and *bnip1b*, map to zebrafish chromosomes 14 and 21, respectively (Table S1). Both *bnip1a* and *bnip1b* mRNAs were expressed ubiquitously during the gastrulation stages, and predominantly in the head, including the retina, after 24 hpf (Figure S3A). We generated antibodies against zebrafish BNip1a and BNip1b, which are applicable for western blotting (Figure S3B) and immunohistochemistry (Figure S3C), and examined the subcellular localization of BNip1 proteins in zebrafish retinal cells. The expression patterns of both BNip1 proteins overlapped with that observed for the ER marker ER-mKO at 24 and 48 hpf (Figures S3D and S3E). It was reported that the ER localization of human BNip1 depends on its transmembrane (TM) domain (Ryu et al., 2012). We found that subcellular localization of zebrafish BNip1 in the ER depends on its TM domain (Figure S3F). Furthermore, using in vitro cultures of human cell lines and an immunoprecipitation assay, we found that zebrafish BNip1a and BNip1b interacted with zebrafish β-SNAP1 (Figure S3G) and zebrafish Bcl2 (Figure S3H). These data suggest that the cellular functions of BNip1 are conserved between zebrafish and humans.

To elucidate whether photoreceptor apoptosis in the *coa* mutant depends on BNip1, we injected morpholino antisense oligonucleotides against BNip1a (MO-BNip1a) and BNip1b (MO-BNip1b) into *coa* mutant embryos. We then examined apoptosis and photoreceptor survival by terminal deoxynucleotidyl transferase-mediated dUTP nick-end labeling (TUNEL) and zpr1 antibody labeling, respectively. Either MO-BNip1a or MO-BNip1b rescued photoreceptors in the *coa* mutant (Figures S4A and S4B). Furthermore, injection of a mixture of both MO-BNip1a and MO-BNip1b more effectively inhibited photoreceptor apoptosis in the *coa* mutant embryos (Figures 3E–3H), although the difference between MO-BNip1b and the mixture of MO-BNip1a and MO-BNip1b was small and not statistically significant (Figure S4B). Because the MO-BNip1a and MO-BNip1b sequences we designed had only seven mismatches out of a total of 25 nucleotides, we used two negative control MOs. One was a special mismatch MO for both BNip1a and BNip1b (mis-MO-BNip1a/b), whose sequence has eight mismatches for MO-BNip1a and six mismatches for MO-BNip1b. The other was a BNip1a-specific MO with five mismatches for MO-BNip1a (5mis-MO-BNip1a) and 11 mismatches for MO-BNip1b. These two control MOs could not rescue photoreceptors in the *coa* mutant (Figures 3E–3H, S4A, and S4B). Furthermore, MO-BNip1a and MO-BNip1b specifically inhibited protein translation of BNip1a and BNip1b, respectively, until 84 hpf (Figure S4C). Taken together, these data suggest that photoreceptor apoptosis in the *coa* mutant depends on BNip1 activity.

Next, we examined whether MO-BNip1 rescues the transport of OS-localized proteins such as peripherin and rhodopsin in the *coa* mutant. In contrast to WT fish and the *coa* mutant expressing β-SNAP1 (Figure 2C), expression of GFP-tagged peripherin and rhodopsin was rescued, but these proteins did not fully accumulate in the apical region of photoreceptors of the *coa* mutant injected with a mixture of both MO-BNip1a and MO-BNip1b (Figure 3I). EM analyses also revealed that MO-BNip1 could not rescue the defects in subcellular morphologies in *coa* mutant photoreceptors (Figures S4D–S4F). Taken together, these data suggest that MO-BNip1 suppresses apoptosis but not the defects in protein transport to the OS in *coa* mutant photoreceptors.

Failed Disassembly of the Syntaxin-18 *cis*-SNARE Complex Causes BNip1-Dependent Apoptosis

SNAP cooperates with NSF to catalyze disassembly of the *cis*-SNARE complex in the vesicular fusion process (Jahn and Scheller, 2006). BNip1 is a t-SNARE component of the syntaxin-18 complex. We hypothesized that failed disassembly of the syntaxin-18 *cis*-SNARE complex increases the levels of the complex, which subsequently activates BNip1-dependent apoptosis. To confirm this hypothesis, we carried out three sets of experiments. The absence of NSF inhibited the disassembly of the *cis*-SNARE complex regardless of the presence of β-SNAP (Figure 4A). Two NSF homologous genes, namely, *nsf-a* and *nsf-b*, were identified in the zebrafish genome (Table S1) (Kurrasch et al., 2009; Woods et al., 2006). First, we examined zebrafish *nsf* mutants. Similar to the case with the *coa*

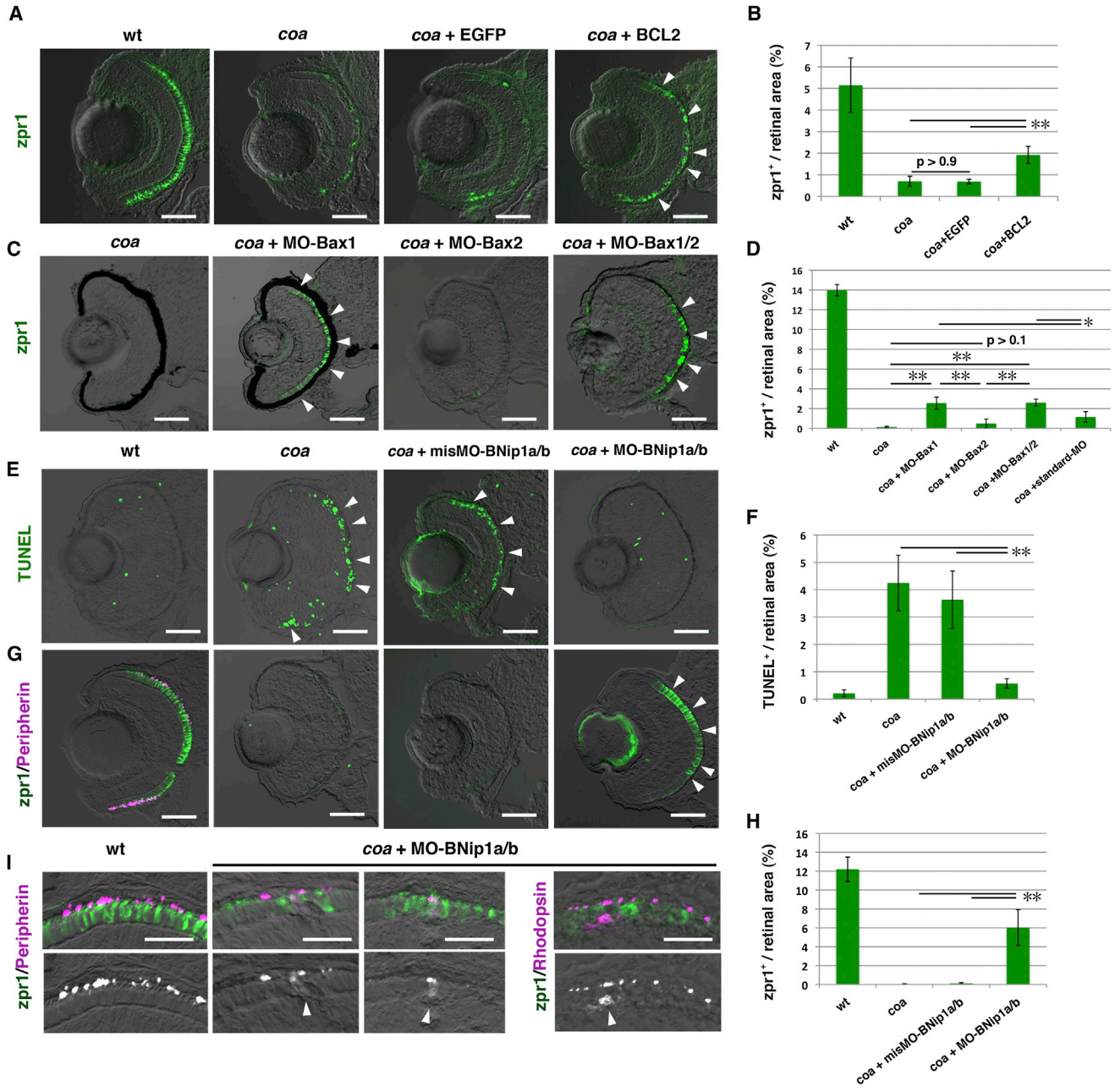

Figure 3. Photoreceptor Degeneration in the *coa* Mutant Depends on BNip1

(A) Zpr1 labeling (green) of 84 hpf WT, *coa* mutants, *coa* mutants injected with *egfp* mRNA, and *bcl2* mRNA. Arrowheads indicate rescued photoreceptors.

(B) Percentage of zpr1-positive areas relative to the total retinal area in the experiments shown in (A). Green and black bars indicate the mean and SD, respectively. **p < 0.01.

(C) Zpr1 labeling (green) of 84 hpf *coa* mutant and *coa* mutants injected with MO-Bax1, MO-Bax2, or a mixture of MO-Bax1 and MO-Bax2. Arrowheads indicate rescued photoreceptors.

(D) Percentage of zpr1-positive areas relative to the total retinal area in the experiments shown in (C) as well as in a *coa* mutant injected with the standard MO. Green and black bars indicate the mean and SD, respectively. **p < 0.01 and *p < 0.05.

(E) TUNEL staining (green) of 84 hpf WT, *coa* mutant, *coa* mutant retinas injected with misMO-BNip1a/b, and a mixture of MO-BNip1a and MO-BNip1b. Arrowheads indicate apoptosis in the ONL.

(F) Percentage of TUNEL-positive areas relative to the total retinal area in the experiments shown in (E). Green and black bars indicate the mean and SD, respectively. **p < 0.01.

(G) Zpr1 labeling (green) and GFP-tagged peripherin (magenta) in 84 hpf WT, *coa* mutant, *coa* mutant retinas injected with misMO-BNip1a/b or a mixture of MO-BNip1a and MO-BNip1b. Arrowheads indicate rescued photoreceptors. Nonspecific zpr1 signal was observed in the lens.

(H) Percentage of zpr1-positive areas relative to the total retinal area in the experiments shown in (G). Green and black bars indicate the mean and SD, respectively. **p < 0.01.

(legend continued on next page)

mutant, severe apoptosis was observed in photoreceptors of zebrafish *nsf-a* mutants at 72 hpf (Figures 4B and 4C). On the other hand, photoreceptors were maintained until 5 dpf in the *nsf-b* mutant, although the *nsf-b* mutant embryos showed abnormal morphologies at 48 hpf (data not shown). Thus, we focused on the *nsf-a* mutant and examined whether photoreceptor apoptosis in the *nsf-a* mutant was dependent on BNip1. Injection of a mixture of MO-BNip1a and MO-BNip1b inhibited photoreceptor apoptosis in *nsf-a* mutants (Figures 4B–4E), suggesting that the blockade of NSF induces BNip1-dependent photoreceptor apoptosis.

Second, we examined whether the knockdown of other components of the syntaxin-18 SNARE complex inhibits photoreceptor apoptosis in the *coa* mutant. In zebrafish, *syntaxin-18* and *use1* genes are annotated as t-SNAREs, and two Sec22b homolog genes, namely, *sec22ba* and *sec22bb*, are annotated as v-SNAREs of the sytaxin-18 complex (Table S1). Sly1 is a Sec1/Munc18 (SM) family protein that regulates the docking and fusion processes of transport vesicles (Carr and Rizo, 2010). Zebrafish *sly1* gene was annotated in the zebrafish genomic database (Table S1). In our model (Figure 4A), knockdown of syntaxin-18 or Use1 inhibits the formation of the syntaxin-18 acceptor SNARE complex, and knockdown of Sec22b and Sly1 inhibits the docking of transport vesicles. It is predicted, then, that both cases would compromise the formation of the syntaxin-18 *cis*-SNARE complex. Injection of morpholinos against syntaxin-18, Use1, Sec22ba, or Sly1 rescued photoreceptors in the *coa* mutant (Figures 4F and 4G), whereas these morpholinos at the same concentration did not affect photoreceptor maintenance in WT (data not shown). Furthermore, injection of either their 5mis-MOs or morpholino against syntaxin 5a-like (MO-Stx5al), a zebrafish homolog of syntaxin 5 that functions in anterograde transport from the ER to Golgi (Jahn and Scheller, 2006), failed to rescue photoreceptors in the *coa* mutant (Figures 4F and 4G). These data suggest that the blockade of formation of the syntaxin-18 *cis*-SNARE complex inhibits BNip1-mediated apoptosis even in the absence of β-SNAP activity.

Third, we examined the level of the syntaxin-18 *cis*-SNARE complex. In a previous study (Fasshauer et al., 2002), it was reported that the *cis*-SNARE complex of the synapse SNARE was stably detected by western blotting of protein extract subjected to heat treatment at <85°C, but dissociated following heat treatment at 100°C. We confirmed that this method successfully detected the *cis*-SNARE complex of the synapse SNARE in zebrafish (see Supplemental Experimental Procedures; Figures S5A and S5B). This western blotting method using the anti-BNip1a and anti-BNip1b antibodies in the long-exposure condition revealed that two bands corresponding to 150 and 100 kDa were detected following heat treatment at 70°C, but disappeared following heat treatment at 100°C (Figure S5C; data not shown). Similar to the case with the *coa* mutant, photoreceptors underwent apoptosis in the *nsf-a* mutant, suggesting that the syntaxin-18 *cis*-SNARE complex is a substrate of NSF-a. Next, we examined whether both 150 and 100 kDa bands are related to the syntaxin-18 *cis*-SNARE complex, in which case their levels would increase in parallel with the reduction in NSF-a activity. Indeed, western blotting using anti-BNip1b antibody revealed that the levels of both bands were increased in 2 dpf *nsf-a* morphant embryos (Figures S5C–S5E). Their levels in the *nsf-a* morphant were decreased by morpholino-mediated knockdown of Sec22ba (Figures S5C–S5E), syntaxin-18 (Figures S5F and S5G), Use1 (Figures S5H and S5I), and BNip1b (Figures S5J and S5K), suggesting that both bands are associated with syntaxin-18, BNip1b, Use1, and Sec22ba. Furthermore, using anti-sec22L1 antibody, which recognizes zebrafish Sec22ba (Figure S4C), we obtained similar results from western blotting of 2 dpf WT, *nsf-a* morphant, and *nsf-a* and *sec22ba* double-morphant embryos (Figures S5L and S5M). These data indicated that both 150 and 100 kDa bands are accumulated in association with the reduction of NSF activity, and that this accumulation depends on syntaxin-18 SNARE component activities. Since the total molecular weight of the syntaxin-18 SNARE complex is estimated to be 117.1 kDa (syntaxin-18, 36.3 kDa; BNip1b, 26.5 kDa; Use1, 29.9 kDa; Sec22ba, 24.4 kDa), we consider it likely that the 100-kDa band contains the syntaxin-18 *cis*-SNARE complex. Taken together, these data suggest that failed disassembly of the syntaxin-18 *cis*-SNARE complex causes BNip1-mediated apoptosis in zebrafish photoreceptors.

Concurrent Expression of Syntaxin-18 SNARE Components Induces Bax-Dependent Apoptosis in a BNip1-BH3-Domain-Dependent Manner

Previous studies have demonstrated that overexpression of BNip1 results in moderate proapoptotic activity that is less efficient than other proapoptotic Bcl2 proteins (Nakajima et al., 2004; Yasuda and Chinnadurai, 2000). This is consistent with the idea that BNip1 proapoptotic activity is activated through the formation of the syntaxin-18 *cis*-SNARE complex. To confirm this, we examined whether concurrent expression of other syntaxin-18 SNARE components facilitates BNip1 proapoptotic activity. We injected an mRNA mixture of all four syntaxin-18 SNARE components into zebrafish eggs and examined their effects on apoptosis during the early stages of development. Embryos injected with an mRNA mixture of all four syntaxin-18 SNARE components showed an increase in the number of apoptotic cells positive for activated caspase 3 (Figure 5A) and TUNEL (data not shown) at 7 hpf, resulting in embryonic death and morphological defects at 8 hpf (Figures 5B–5D). In contrast, apoptosis and morphological abnormalities decreased in embryos injected with an mRNA mixture of three syntaxin-18 SNARE components lacking *bnip1b* (Figures 5A–5D), *syntaxin-18*, *use1*, or *sec22ba* (Figures S6A–S6C), or two mRNA combinations of *bnip1b* with *syntaxin18*, *use1*, or *sec22ba* (Figures S6B and S6C; data not shown). We also examined whether coexpression of β-SNAP1 could prevent syntaxin-18 SNARE-induced apoptosis. In contrast to the

(I) Zpr1 labeling (green) and GFP-tagged peripherin or rhodopsin (magenta) in the photoreceptor cell layer in WT and *coa* mutants injected with MO-BNip1a and MO-BNip1b. Lower panels show the magenta channel. Arrowheads indicate the failure of transport to the OS.
The numbers of retinal sections used in the experiments shown in (B), (D), (F), and (H) and p values for the t test are shown in Table S2. Scale bars, 50 μm (A, C, E, and G) and 10 μm (I). See also Figures S3 and S4.

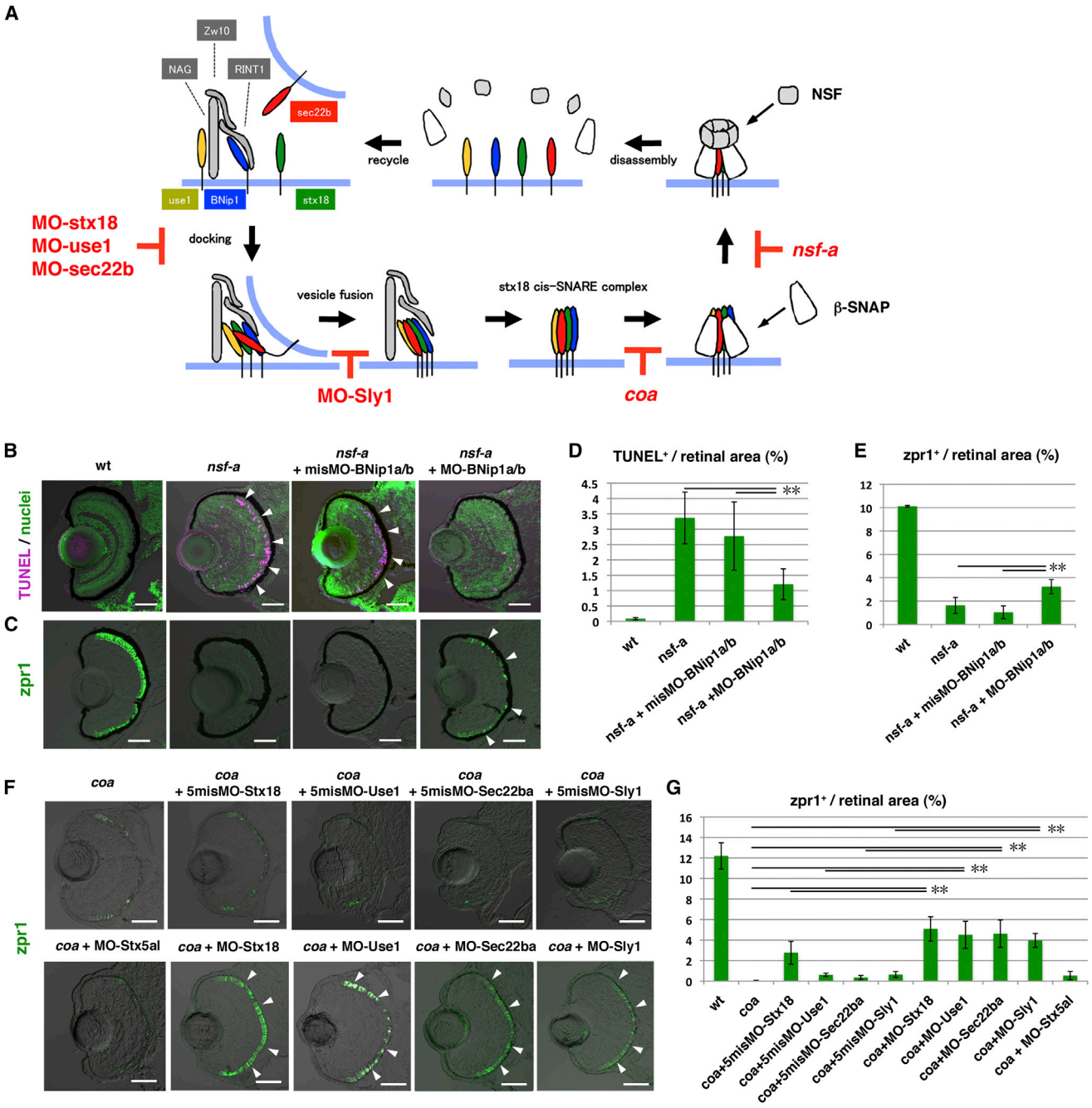

Figure 4. The Syntaxin-18 *cis*-SNARE Complex Is Required for BNip1-Dependent Apoptosis

(A) Molecular mechanism underlying vesicular fusion to the ER. Interactions among syntaxin-18 (green), BNip1 (blue), Use1 (yellow), and Sec22b (red) initiate the fusion of transport vesicles to the ER membrane. Three accessory proteins, Zw10, NAG, and RINT1, play a role in the tethering of transport vesicles. After membrane fusion occurs, β-SNAP binds to the *cis*-SNARE complex and recruits NSF. NSF promotes disassembly of the *cis*-SNARE complex. In the absence of β-SNAP or NSF activity, the syntaxin-18 *cis*-SNARE complex accumulates. MOs against syntaxin-18, Use1, Sec22b, and Sly1 inhibit the formation of the syntaxin-18 *cis*-SNARE complex, even in the absence of β-SNAP or NSF activity.

(B) TUNEL staining (magenta) of 72 hpf WT, *nsf-a* mutant, and *nsf-a* mutant retinas injected with misMO-BNip1a/b, and a mixture of MO-BNip1a and MO-BNip1b. Nuclei were counterstained with SYTOX Green (green). Arrowheads indicate apoptosis in the ONL.

(C) Zpr1 labeling (green) of 84 hpf WT, *nsf-a* mutant, *nsf-a* mutant retinas injected with misMO-BNip1a/b, and a mixture of MO-BNip1a and MO-BNip1b. Arrowheads indicate rescued photoreceptors.

(D and E) Percentage of TUNEL-positive (D) and zpr1-positive areas (E) relative to the total retinal area in the experiments shown in (B) and (C), respectively. Green and black bars indicate the means and SDs, respectively. $^{**}p < 0.01$.

(F) Zpr1 labeling (green) of *coa* mutant and *coa* mutants injected with MO-syntaxin-18, MO-Use1, MO-Sec22ba, MO-Sly1, their 5misMOs, and MO-syntaxin 5al. Arrowheads indicate rescued photoreceptors.

(legend continued on next page)

negative control (*egfp* mRNA), coexpression of *β-snap1* mRNA inhibited syntaxin-18 SNARE-induced apoptosis (Figures S6D–S6F). Thus, these data indicate that the concurrent expression of all four syntaxin-18 SNARE components induces apoptosis in conflict with β-SNAP1 activity.

Next, we examined whether syntaxin-18 SNARE-induced apoptosis is dependent on BNip1 proapoptotic activity. It was previously reported that BNip1 binds to Bcl2 and Bcl-XL through its BH3 domain, which may liberate Bax (Yasuda and Chinnadurai, 2000; Zhang et al., 1999). Leu-114 of the BNip1-BH3 domain corresponds to the most conserved residue in the core BH3 domain, which is important for the interaction of the BH3 domain with Bcl2 family proteins (Lomonosova and Chinnadurai, 2008). Indeed, the missense mutation of Leu-114 to Ala reduces the proapoptotic activity of BNip1 in humans (Nakajima et al., 2004). The replacement of WT BNip1b with BNip1b carrying the L114A mutation (BNip1b(L114A)) did not affect the protein expression level (Figure S6G), but it did reduce syntaxin-18 SNARE-mediated apoptosis (Figures 5A–5D). Furthermore, a mixture of MO-Bax1 and MO-Bax2 inhibited syntaxin-18 SNARE-mediated apoptosis (Figures 5A–5D). MO-Bax2 inhibited apoptosis to a level similar to what was observed with a mixture of MO-Bax1 and MO-Bax2, whereas MO-Bax1 inhibited it less efficiently. Because *bax2* mRNA is expressed mainly in the early stage (Kratz et al., 2006), Bax2 predominantly mediates apoptosis at 7 hpf. Taken together, these data suggest that concurrent expression of all syntaxin-18 SNARE components induces Bax-dependent apoptosis in a BNip1-BH3 domain-dependent manner.

Next, we examined whether concurrent expression of the syntaxin-18 SNARE components would induce apoptosis in zebrafish retinal neurons. We injected WT eggs with a mixture of five DNA constructs, encoding syntaxin-18, BNip1b, Use1, Sec22ba, and EGFP, under the control of the retinal enhancer of the *atoh7* gene (Masai et al., 2003). This *atoh7* enhancer drives expression in all differentiating retinal neurons (Poggi et al., 2005) as well as anterior commissural (AC) and olfactory neurons. We selected embryos that highly expressed GFP in the retina, and performed TUNEL staining in 48 and 72 hpf retinas. Apoptosis occurred specifically in GFP-labeled retinal neurons as well as in AC and olfactory neurons (Figure 5E). Their apoptotic levels were consistent with our estimation of concurrent expression (see Supplemental Experimental Procedures; Figures S6H and S6I; Table S3). On the other hand, such apoptosis was not observed in retinal neurons expressing only EGFP (Figures 5E and 5F). These data suggest that concurrent expression of all syntaxin-18 SNARE components induces apoptosis in differentiating retinal neurons in zebrafish.

The N-Terminal Coiled-Coil Domain Suppresses BNip1 Proapoptotic Activity

Although concurrent expression of all syntaxin-18 SNARE components effectively induces apoptosis, expression of *bnip1b* mRNA alone did not induce apoptosis (Figure 6). This suggests that BNip1's proapoptotic activity is absent when BNip1 does not form the *cis*-SNARE complex. BNip1 consists of a coiled-coil domain, the BH3 domain, a SNARE domain, and a TM domain (Figure 6A). To examine whether BNip1 proapoptotic activity is modulated by these domains, we focused on BNip1b and made expression DNA constructs of three deletion mutants: BNip1b-ΔTM, BNip1b-ΔSNARE, and BNip1b-Δcc. These mutants lack the TM domain, both the SNARE and TM domains, and both the coiled-coil and TM domains, respectively (Figure 6A). Because the BNip1 TM domain is required for ER localization (Figure S3F), deletion of the TM domain is thought to minimize the interaction between modified BNip1 proteins and other syntaxin-18 SNARE components in the ER. All of these deletion proteins were expressed at 7 hpf (Figure S7A), and their subcellular localizations were ubiquitous (Figure S7B). Injection of mRNA encoding BNip1b-ΔTM into zebrafish eggs induced apoptosis and morphological defects very mildly (Figures 6B–6D). Injection of mRNA encoding BNip1b-ΔSNARE did not induce apoptosis or morphological defects (Figures 6B–6D). On the other hand, injection of mRNA encoding BNip1b-Δcc induced apoptosis and embryonic death much more severely compared with BNip1b-ΔTM (Figures 6B–6D), suggesting that deletion of the coiled-coil domain enhanced apoptosis caused by BNip1bΔTM.

Next, we examined whether BNip1b-Δcc-mediated apoptosis depends on Bax and the BNip1-BH3 domain. Coinjection of MO-Bax2 inhibited BNip1-Δcc-mediated apoptosis, whereas MO-Bax1 inhibited it less effectively (Figures S7C–S7E). Furthermore, the amino acid substitution L114A in the BH3 domain or deletion of the BH3 domain reduced BNip1b-Δcc-mediated apoptosis, although the difference between BNip1b-Δcc and BNip1b-Δcc(L114A) was not statistically significant (Figures 6B–6D). These data suggest that, similarly to syntaxin-18 SNARE-mediated apoptosis, BNip1b-Δcc induces Bax2-dependent apoptosis in a BNip1-BH3-dependent manner. Taken together, these data suggest that deletion of the coiled-coil domain of BNip1b induces Bax-dependent apoptosis in a BH3 domain-dependent manner.

DISCUSSION

In this study, we showed that *β-snap1* mutation causes BNip1-dependent apoptosis in zebrafish *coa* mutant photoreceptors. BNip1 is a t-SNARE component of the syntaxin-18 complex. We showed that the failed disassembly of the syntaxin-18 *cis*-SNARE complex is responsible for BNip1-dependent apoptosis. In this context, the syntaxin-18 *cis*-SNARE complex is an indicator of vesicular fusion defects, and BNip1 transforms vesicular fusion defects into apoptosis. It is likely that vesicular fusion defects caused by *β-snap1* mutation compromise the recycling of SNAREs and eventually arrest intracellular vesicular transport. It was previously reported that a failure in the transport of rhodopsin to the OS is associated with photoreceptor degeneration (Mendes et al., 2005). In *coa* mutant photoreceptors, the

(G) Percentage of zpr1-positive area relative to the total retinal area in the experiments shown in (F). Green and black bars indicate the means and SDs, respectively (**$p < 0.01$).

The numbers of retinal sections used in the experiments shown in (D), (E), and (G) and p values for the t test are shown in Table S2. Scale bars, 50 μm. See also Figure S5.

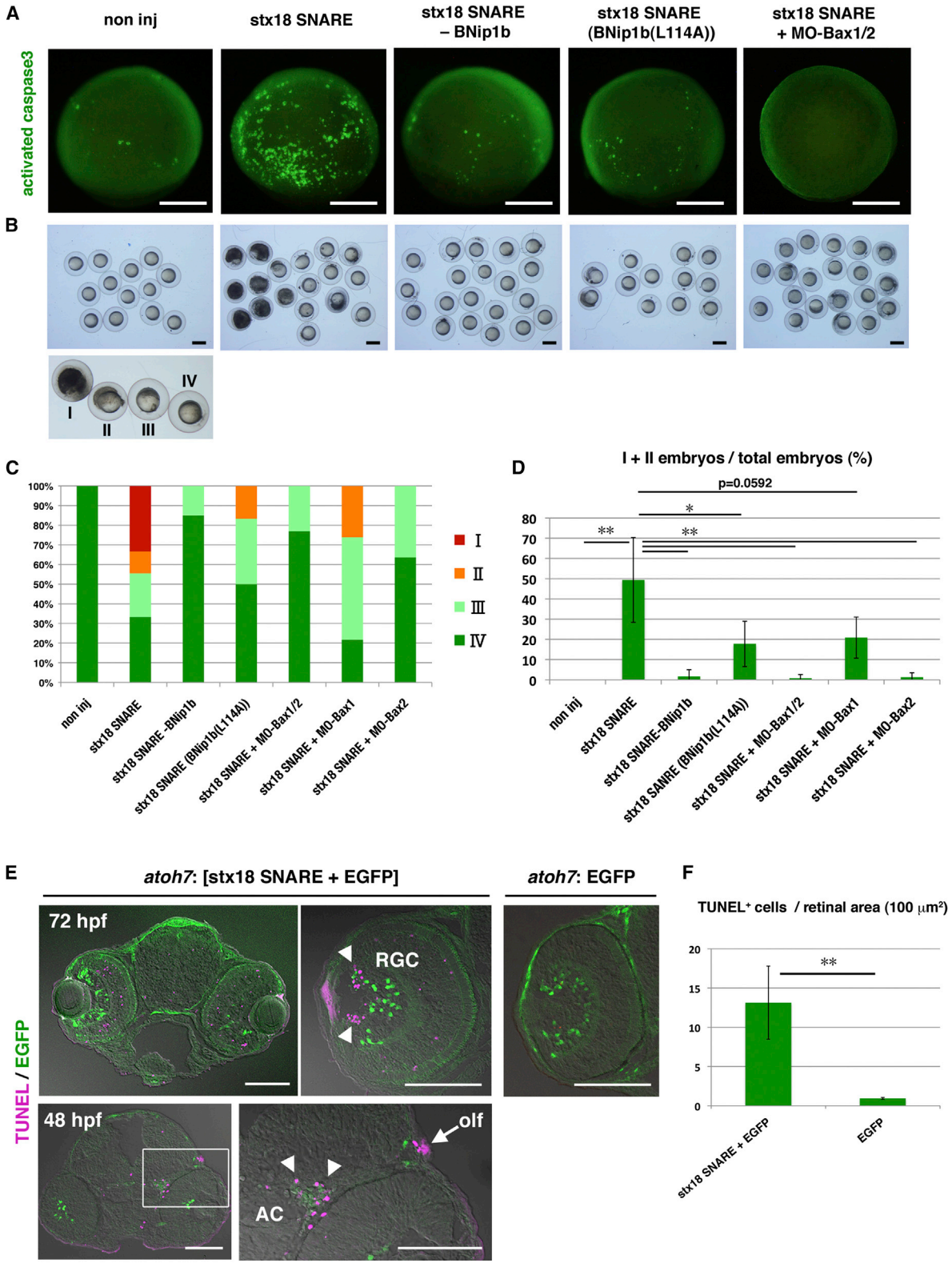

Figure 5. Concurrent Expression of Syntaxin-18 SNARE Components Induces Bax-Dependent Apoptosis in a BNip1-BH3 Domain-Dependent Manner

(A) Antiactivated caspase 3 antibody labeling of 7 hpf embryos injected with different RNA combinations of syntaxin-18 SNARE components: noninjection, syntaxin-18 SNARE mixture, syntaxin-18 SNARE mixture lacking BNip1b, syntaxin-18 SNARE mixture replaced with BNip1b (L114A), and syntaxin-18 SNARE

(legend continued on next page)

knockdown of BNip1 rescued photoreceptors but failed to recover transport of rhodopsin to the OS. These data suggest that rhodopsin transport defects are not a primary cause of the photoreceptor degeneration in the *coa* mutant, and that a BNip1-dependent apoptotic pathway is activated in response to vesicular fusion defects prior to the photoreceptor degeneration caused by rhodopsin transport defects.

Our findings suggest that the level of syntaxin-18 *cis*-SNARE complex on the ER is critical for the decision as to whether photoreceptors will survive or undergo apoptosis. Defects in budding of transport vesicles or their docking to target membranes lead to a failure to initiate vesicular fusion, resulting in reduced *cis*-SNARE complex formation. Thus, it appears that *cis*-SNARE complexes are not accumulated when vesicular fusion fails to be initiated. Rather, *cis*-SNARE complexes are accumulated only when vesicular-fusion-mediated SNARE assembly is higher than SNAP/NSF-mediated SNARE disassembly. However, it is expected that the defects in SNAP/NSF-mediated SNARE disassembly reduce the recycling of SNAREs, which in turn inhibits new vesicular fusion and subsequent *cis*-SNARE complex formation. Thus, the balance between assembly and disassembly of SNAREs may be automatically maintained by this SNARE recycling system. Why is the syntaxin-18-mediated apoptotic pathway necessary, especially in photoreceptors? In the *coa* mutant, photoreceptor apoptosis occurred mostly in the period from 48 to 84 hpf. During this period, large amounts of photoreceptive proteins and membrane components are transported from the ER to the OS, resulting in very active vesicular transport. Because SNAP functions as a noncatalytic adaptor between all *cis*-SNARE complexes and NSF, excessive activation of vesicular transport is likely to increase the frequency of vesicular fusion events, resulting in the consumption of all available SNAP. It is possible that the conventional SNARE recycling system is unable to ensure such active vesicular transport, and that the syntaxin-18 *cis*-SNARE complex is necessary as an additional vesicular transport quality-control step for monitoring the availability of SNAP during photoreceptor differentiation. Because the available amounts of SNAP represent vesicular fusion competence, the syntaxin-18 *cis*-SNARE complex may sense vesicular fusion competence on the ER membrane during photoreceptor differentiation.

Among all the members of the diverse SNARE protein family, BNip1 is the only SNARE that harbors the BH3 domain. Why is the syntaxin-18 *cis*-SNARE complex selected as the sensor of vesicular fusion competence? The syntaxin-18 SNARE complex regulates retrograde transport from the Golgi to the ER. Because retrograde transport retrieves ER-resident proteins that have escaped the ER by anterograde transport, the level of retrograde transport may be in proportion to that of anterograde transport. If this is the case, the amount of the syntaxin-18 *cis*-SNARE complex on the ER membrane could be an indicator of excessive activation of anterograde transport. The blockade of anterograde transport from the ER to the Golgi causes abnormal accumulation of newly synthesized proteins in the ER, which subsequently activates the ER-stress response. In this context, the syntaxin-18 *cis*-SNARE complex and the ER-stress response cooperatively determine the upper and lower limits of the adequate range of vesicular fusion frequency.

The next important question is, how does formation of the syntaxin-18 *cis*-SNARE complex activate BNip1 proapoptotic activity? In this study, we showed that concurrent expression of all syntaxin-18 SNARE components induced Bax-dependent apoptosis in a BNip1-BH3 domain-dependent manner. Interestingly, expression of BNip1 alone did not induce apoptosis, suggesting that BNip1 proapoptotic activity is absent in the non-*cis*-SNARE state. We found that deletion of the coiled-coil domain enhanced BNip1 proapoptotic activity. It has consistently been reported that deletion of the N-terminal coiled-coil domain increases the binding between BNip1 and BclXL in humans (Yasuda and Chinnadurai, 2000). BNip1 interacts with Bcl2 and BclXL through its BH3 domain (Yasuda and Chinnadurai, 2000; Zhang et al., 1999), which may liberate Bak/Bax. Alternatively, BNip1 may directly activate Bax through its BH3 domain, although the binding affinity of BNip1 for Bax is much lower than that of BNip1 for Bcl2/Bcl-XL (Zhang et al., 1999). We showed that zebrafish BNip1a/b interact physically with zebrafish Bcl2, and that BNip1b-Δcc-mediated apoptosis depends on Bax and the BNip1 BH3 domain. One possible model is that the coiled-coil domain directly or indirectly reduces the affinity between the BH3 domain and Bcl2, and that syntaxin-18 *cis*-SNARE complex formation triggers a conformational change in BNip1, which enables the BH3 domain to interact with Bcl2 (Figure 7). In this context, BNip1 proapoptotic activity is inhibited by two distinct mechanisms depending on the BNip1 state. In the monomer state or the SNARE acceptor complex state, the coiled-coil domain suppresses BNip1 proapoptotic activity. In the *cis*-SNARE complex state, SNAP/NSF-mediated disassembly of the *cis*-SNARE complex suppresses

mixture plus a mixture of MO-Bax1 and MO-Bax2. Cells with active caspase 3 were increased only in embryos injected with a mixture of mRNAs for all four syntaxin-18 SNARE components.

(B) Top panels indicate 8 hpf embryos injected with the same RNA combinations shown in (A). The bottom panel shows a classification of the morphological defects of 8-hpf-injected embryos as embryonic cell death (class I), blown-up blastoderm during gastrulation (class II), nonuniform thickness of the blastoderm (class III), and normal morphology (class IV).

(C) Percentages of 8 hpf embryos classified as classes I–IV in the injection experiments shown in (B) as well as the injection experiments for the syntaxin-18 SNARE mixture plus either MO-Bax1 or MO-Bax2.

(D) Percentage of class I/II embryos. Green and black bars indicate the mean and SD, respectively. The numbers of injection experiments and t test p values are shown in Table S2. *$p < 0.05$, **$p < 0.01$.

(E) TUNEL staining of WT embryos expressing a mixture of all syntaxin-18 SNARE components and EGFP or only EGFP under the control of the *atoh7* retinal enhancer. In embryos expressing a mixture of all syntaxin-18 SNARE components and EGFP, TUNEL-positive cells (magenta) are observed in the GFP-positive (green) retinal region, especially retinal ganglion cells (RGC; arrowheads), and anterior commissural (AC, arrowheads) and olfactory (olf, arrow) neurons.

(F) The density of apoptotic cells (number/100 μm^2) in retinas injected with DNA constructs encoding a mixture of syntaxin-18 SNARE components and EGFP or only EGFP. The number of examined retinas was n = 4 for each. Green and black bars indicate the mean and SD; **$p < 0.01$.

Scale bars, 200 μm (A), 600 μm (B), and 50 μm (E). See also Figure S6.

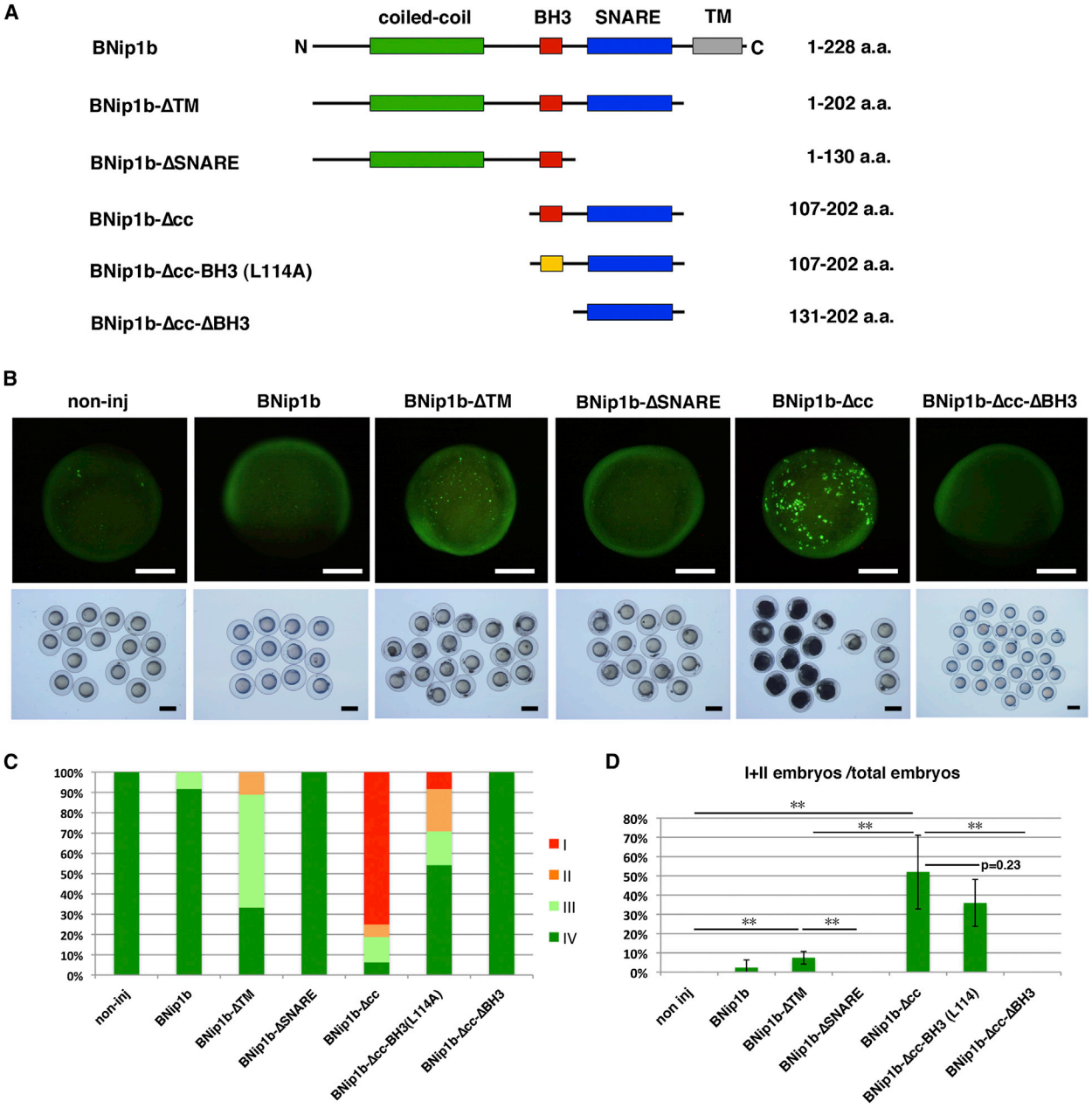

Figure 6. The N-Terminal Coiled-Coil Domain Suppresses BNip1 Proapoptotic Activity

(A) BNip1b has four distinct domains: a coiled-coil domain, a BH3 domain, a SNARE domain, and a TM domain. Configuration of deletion constructs (BNip1b-ΔTM, BNip1b-ΔSNARE, BNip1b-Δcc, BNip1b-Δcc-BH3(L114A), and BNip1b-Δcc-ΔBH3).

(B) Activation of caspase 3 at 7 hpf (upper rows) and morphologies at 8 hpf (lower rows) in embryos injected with mRNA encoding BNip1b, BNip1b-ΔTM, BNip1b-ΔSNARE, BNip1b-Δcc, and BNip1b-Δcc-ΔBH3. Severe embryonic death and morphological defects are observed only in BNip1Δcc-expressing embryos.

(C) Percentages of 8 hpf embryos classified as classes I–IV in the injection experiments shown in (B) (lower panels), as well as BNip1b-Δcc-BH3(L114A).

(D) Percentage of class I/II embryos. Green and black bars indicate the means and SDs, respectively. The numbers of injection experiments and t test p values are shown in Table S2. **$p < 0.01$.

Scale bars, 200 μm (B, upper panels) and 600 μm (B, lower panels). See also Figure S7.

BNip1 proapoptotic activity. The latter mechanism is linked to sensing of vesicular fusion competence.

In summary, we have identified a surveillance mechanism for monitoring vesicular fusion competence in photoreceptors. In the future, it will be important to elucidate signaling pathways downstream of BNip1 activation on the ER, for example, to determine whether BNip1 interacts with Bcl2/BclXL on the ER membrane, and how sequestering of Bcl2/BclXL by BNip1 on

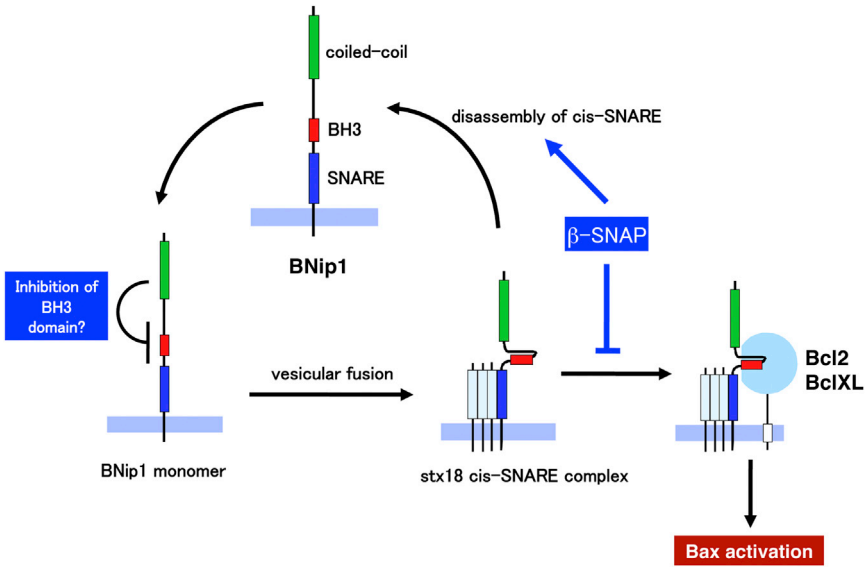

Figure 7. Possible Mechanism Underlying BNip1-Dependent Apoptosis

BNip1 proapoptotic activity depends on the BH3 domain, but is normally inactivated by the N-terminal coiled-coil domain. Fusion of retrograde transport vesicles to the ER membrane results in the formation of the syntaxin-18 *cis*-SNARE complex, which enables the BH3 domain to interact with Bcl2. The interaction of BNip1 with Bcl2 may release Bax, or BNip1 may directly activate Bax to promote apoptosis. β-SNAP1 inhibits BNip1-dependent apoptosis by disassembling the syntaxin-18 *cis*-SNARE complex.

the ER promotes apoptosis. Furthermore, many hereditary retinal diseases that cause photoreceptor degeneration have been identified in humans. It will be interesting to examine which hereditary retinal diseases are linked to dysfunction of SNAP/NSF and BNip1-dependent photoreceptor degeneration. In such cases, the development of innovative drugs that can inhibit BNip1 may contribute to the establishment of therapies for human patients.

EXPERIMENTAL PROCEDURES

Fish Strain

Zebrafish (*Danio rerio*) were maintained according to standard procedures (Westerfield, 1995). The WT and mutant strains used in this study are described in the Supplemental Experimental Procedures.

Histology

Antibody labeling, in situ hybridization, cryosectioning, plastic sectioning, and cell transplantation were performed as described previously (Masai et al., 2003). The antibodies we used in this study were zpr1 (1:100; Oregon Monoclonal Bank) and anti-zebrafish rhodopsin, red opsin, green opsin, blue opsin, and UV opsin (1:50–500; Vihtelic et al., 1999). Labeling with SYTOX Green (Molecular Probes; 50–100 nM) was carried out as previously described (Masai et al., 2003). TUNEL and EM analyses were carried out as previously described (Nishiwaki et al., 2008).

Microinjection of DNA, RNA, and Morpholinos into Zebrafish Embryos

Details regarding the procedures used for DNA construction and microinjection are described in the Supplemental Experimental Procedures. Microinjection of morpholino antisense oligos was carried out as described in the Supplemental Experimental Procedures.

Selection of *coa* and *nsf* Mutant Embryos

Although *nsf-a* homozygous mutants showed excessive expansion of melanophore pigmentation at 4 dpf, both *coa* and *nsf-a* homozygous mutant embryos were indistinguishable from their WT siblings in terms of external morphology until 3 dpf. Thus, in all of the experiments in this study, both *coa* and *nsf-a* homozygous mutant embryos were selected by genotyping. Because *nsf-b* homozygous mutants display defects in external morphology and less-developed melanophores after 2 dpf, *nsf-b* homozygous mutant embryos were selected based on these morphological defects. To select transgenic embryos carrying GFP-tagged peripherin under the control of the *Xenopus rhodopsin* promoter, embryos were incubated with phenylthiourea at a final concentration of 0.003% (w/v) to prevent retinal pigmentation. For genotyping, embryos were generated by pairwise crosses of heterozygous mutant fish and fixed in 4% (w/v) paraformaldehyde (PFA) at the appropriate stages. Heads and bodies were separated. Genomic DNA was prepared from individual bodies and their genotypes were determined by PCR using specific polymorphic markers. Heads of WT and homozygous mutants were used for further histological, western blotting, and biochemical experiments.

Expression of Syntaxin-18 SNARE Components

Full-length *syntaxin-18*, *bnip1b*, *use1*, and *sec22ba* complementary DNAs (cDNAs) were subcloned into the pCS2 vector and used to generate mRNAs by in vitro transcription reactions. An mRNA mixture of different SNARE combinations (50 μg/mL each) was injected into zebrafish eggs. *β-snap1* and *egfp* mRNAs were used at 200 μg/mL for coinjection with syntaxin-18 SNARE mRNAs. cDNAs for the BNip1b deletion mutants BNip1b-ΔTM, BNip1b-ΔSNARE, BNip1b-Δcc, and BNip1b-Δcc-ΔBH3 were amplified by PCR using specific primers and subcloned into the pCS2 vector. mRNAs for these BNip1b deletion mutants (800 μg/mL) were injected into zebrafish eggs. Embryos injected at 7 hpf were fixed with 4% (w/v) PFA and used for labeling with antiactivated caspase 3 antibody as previously described (Kratz et al., 2006). For expression of syntaxin-18 SNARE components in retinal cells, we made five DNA constructs encoding syntaxin-18, BNip1b, Use1, Sec22ba, and EGFP under the control of the *atoh7* retinal enhancer. A mixture of these five DNA constructs (final concentrations: 15 μg/mL for *egfp*, and 2.5 μg/mL each for *syntaxin-18*, *bnip1b*, *use1*, and *sec22ba*) was injected into zebrafish WT eggs, and embryos that showed a high level of GFP expression in the retina were fixed with PFA at 48 and 72 hpf and used for TUNEL staining. As a negative control, the DNA construct encoding EGFP under the control of the *atoh7* enhancer was used at 15 μg/mL. Estimation of concurrent expression of the five DNA constructs is described in the Supplemental Experimental Procedures.

Expression of Golgi-GFP, ER-mKO, and GFP-Tagged BNip1b Deletion Mutant Proteins

For construction of Golgi-GFP, the DNA fragment encoding the N-terminal 100 amino acids of mannosidase2A was amplified by PCR and fused to GFP. ER-mKO was originally derived from the ER-targeted peptide sequence from calreticulin. A DNA fragment encoding ER-mKO was taken from the plasmid pER-mKO1 (Medical & Biological Laboratories) and subcloned into the pCS2 expression vector. DNA fragments encoding zebrafish BNip1b, BNip1b-ΔTM, BNip1b-Δcc, and BNip1b-ΔSNARE were fused to the 3′ end of a DNA encoding EGFP in flame, and subcloned into the pCS2 expression vector. The mRNAs encoding Golgi-GFP, ER-mKO, and GFP-tagged deletion mutant BNip1b were synthesized in vitro using the mMESSAGE mMACHINE kit (Ambion). Golgi-GFP and ER-mKO mRNAs were injected into zebrafish eggs at 100 and 200 μg/mL, respectively. At 60 and 72 hpf, the retinas of these

injected embryos were scanned using an LSM510 confocal microscope (Carl Zeiss). GFP-tagged deletion mutant BNip1b mRNAs were injected into zebrafish eggs at 200 μg/mL, and scanned at 7 and 24 hpf using an LSM510 confocal microscope.

Western Blotting

Embryonic heads or adult brain tissues were dissected and used for western blotting as described previously (Tolar and Pallanck, 1998). Antibodies against the peptide sequence of zebrafish BNip1a (amino acids 111–125: KEDLLNSEDMSVRHR) and BNip1b (amino acids 111–124: KDELLQGGDAVRQR) were generated using synthetic peptides and used for western blotting at 1:500–1:1,000. Anti-GFP antibody (MBL), anti-syntaxin 1 antibody (ab39986; Abcam), anti-SNAP25 (ab41455; Abcam), and anti-Sec22L1 antibody (ab68835; Abcam) were used at 1:5,000, 1:20,000, 1:770, and 1:500, respectively. Signals were developed using ImmunoStar LD (Wako). Luminescence was quantified using a Fuji LAS-4000mini image analyzer (Fuji Film). The syntaxin-18 *cis*-SNARE complex was detected as described in the Supplemental Experimental Procedures.

Calculation of the Percentage of TUNEL- and zpr1-Positive Areas Relative to the Total Retinal Area

Cryosections labeled with TUNEL or zpr1 antibody were scanned under a laser-scanning microscope (LSM510; Carl Zeiss). The percentage of TUNEL- or zpr1-positive areas relative to the total retinal area was determined using a one-section image containing the central retina per eye. The means and standard deviations were calculated from data obtained for two to ten sections from more than two embryos. The numbers of sections used and the results of a Student's t test are shown in Table S2. Using ImageJ software (NIH), we converted TUNEL- or zpr1-positive and -negative areas to a binary scale with two digits (1 and 0, respectively). The number of pixels corresponding to 1 or 0 within the neural retina was determined. The percentage of TUNEL- or zpr1-positive areas relative to the total retinal area was calculated as the percentage of 1 pixels relative to the number of 0+1 pixels.

SUPPLEMENTAL INFORMATION

Supplemental Information includes Supplemental Experimental Procedures, seven figures, and three tables and can be found with this article online at http://dx.doi.org/10.1016/j.devcel.2013.04.015.

ACKNOWLEDGMENTS

We thank Dr. A. Thomas Look for providing the DNA construct for Bcl2, Dr. Robert S. Molday for providing the DNA construct for *Xenopus*-peripherin-2-GFP under the control of the *Xenopus* rhodopsin promoter, and Dr. David R. Hyde for providing anti-zebrafish opsin antibodies. We thank Yayoi Tomoyose, Ayako Nameki, Kazumi Toguchi, Yuko Yamazato, and Yuki Tamae for fish facility support. This work was supported by grants from OIST to I.M. and from MEXT to I.M. and Y.N. (23650173).

Received: June 29, 2012
Revised: March 15, 2013
Accepted: April 27, 2013
Published: May 28, 2013

REFERENCES

Aoki, T., Kojima, M., Tani, K., and Tagaya, M. (2008). Sec22b-dependent assembly of endoplasmic reticulum Q-SNARE proteins. Biochem. J. *410*, 93–100.

Babcock, M., Macleod, G.T., Leither, J., and Pallanck, L. (2004). Genetic analysis of soluble N-ethylmaleimide-sensitive factor attachment protein function in Drosophila reveals positive and negative secretory roles. J. Neurosci. *24*, 3964–3973.

Bonifacino, J.S., and Glick, B.S. (2004). The mechanisms of vesicle budding and fusion. Cell *116*, 153–166.

Boyd, J.M., Malstrom, S., Subramanian, T., Venkatesh, L.K., Schaeper, U., Elangovan, B., D'Sa-Eipper, C., and Chinnadurai, G. (1994). Adenovirus E1B 19 kDa and Bcl-2 proteins interact with a common set of cellular proteins. Cell *79*, 341–351.

Burgalossi, A., Jung, S., Meyer, G., Jockusch, W.J., Jahn, O., Taschenberger, H., O'Connor, V.M., Nishiki, T., Takahashi, M., Brose, N., and Rhee, J.S. (2010). SNARE protein recycling by αSNAP and βSNAP supports synaptic vesicle priming. Neuron *68*, 473–487.

Carr, C.M., and Rizo, J. (2010). At the junction of SNARE and SM protein function. Curr. Opin. Cell Biol. *22*, 488–495.

Clary, D.O., and Rothman, J.E. (1990). Purification of three related peripheral membrane proteins needed for vesicular transport. J. Biol. Chem. *265*, 10109–10117.

Clary, D.O., Griff, I.C., and Rothman, J.E. (1990). SNAPs, a family of NSF attachment proteins involved in intracellular membrane fusion in animals and yeast. Cell *61*, 709–721.

Deretic, D., Schmerl, S., Hargrave, P.A., Arendt, A., and McDowell, J.H. (1998). Regulation of sorting and post-Golgi trafficking of rhodopsin by its C-terminal sequence QVS(A)PA. Proc. Natl. Acad. Sci. USA *95*, 10620–10625.

Eley, L., Yates, L.M., and Goodship, J.A. (2005). Cilia and disease. Curr. Opin. Genet. Dev. *15*, 308–314.

Fasshauer, D., Antonin, W., Subramaniam, V., and Jahn, R. (2002). SNARE assembly and disassembly exhibit a pronounced hysteresis. Nat. Struct. Biol. *9*, 144–151.

Hatsuzawa, K., Hirose, H., Tani, K., Yamamoto, A., Scheller, R.H., and Tagaya, M. (2000). Syntaxin 18, a SNAP receptor that functions in the endoplasmic reticulum, intermediate compartment, and cis-Golgi vesicle trafficking. J. Biol. Chem. *275*, 13713–13720.

Hirose, H., Arasaki, K., Dohmae, N., Takio, K., Hatsuzawa, K., Nagahama, M., Tani, K., Yamamoto, A., Tohyama, M., and Tagaya, M. (2004). Implication of ZW10 in membrane trafficking between the endoplasmic reticulum and Golgi. EMBO J. *23*, 1267–1278.

Insinna, C., Baye, L.M., Amsterdam, A., Besharse, J.C., and Link, B.A. (2010). Analysis of a zebrafish dync1h1 mutant reveals multiple functions for cytoplasmic dynein 1 during retinal photoreceptor development. Neural Dev. *5*, 12.

Jahn, R., and Scheller, R.H. (2006). SNAREs—engines for membrane fusion. Nat. Rev. Mol. Cell Biol. *7*, 631–643.

Kaiser, C.A., and Schekman, R. (1990). Distinct sets of SEC genes govern transport vesicle formation and fusion early in the secretory pathway. Cell *61*, 723–733.

Kajiwara, K., Sandberg, M.A., Berson, E.L., and Dryja, T.P. (1993). A null mutation in the human peripherin/RDS gene in a family with autosomal dominant retinitis punctata albescens. Nat. Genet. *3*, 208–212.

Kennan, A., Aherne, A., and Humphries, P. (2005). Light in retinitis pigmentosa. Trends Genet. *21*, 103–110.

Kratz, E., Eimon, P.M., Mukhyala, K., Stern, H., Zha, J., Strasser, A., Hart, R., and Ashkenazi, A. (2006). Functional characterization of the Bcl-2 gene family in the zebrafish. Cell Death Differ. *13*, 1631–1640.

Kurrasch, D.M., Nevin, L.M., Wong, J.S., Baier, H., and Ingraham, H.A. (2009). Neuroendocrine transcriptional programs adapt dynamically to the supply and demand for neuropeptides as revealed in NSF mutant zebrafish. Neural Dev. *4*, 22.

Langenau, D.M., Jette, C., Berghmans, S., Palomero, T., Kanki, J.P., Kutok, J.L., and Look, A.T. (2005). Suppression of apoptosis by bcl-2 overexpression in lymphoid cells of transgenic zebrafish. Blood *105*, 3278–3285.

Larison, K.D., and Bremiller, R. (1990). Early onset of phenotype and cell patterning in the embryonic zebrafish retina. Development *109*, 567–576.

Loewen, C.J., Moritz, O.L., Tam, B.M., Papermaster, D.S., and Molday, R.S. (2003). The role of subunit assembly in peripherin-2 targeting to rod photoreceptor disk membranes and retinitis pigmentosa. Mol. Biol. Cell *14*, 3400–3413.

Lomonosova, E., and Chinnadurai, G. (2008). BH3-only proteins in apoptosis and beyond: an overview. Oncogene *27*(*Suppl 1*), S2–S19.

Masai, I., Lele, Z., Yamaguchi, M., Komori, A., Nakata, A., Nishiwaki, Y., Wada, H., Tanaka, H., Nojima, Y., Hammerschmidt, M., et al. (2003). N-cadherin mediates retinal lamination, maintenance of forebrain compartments and patterning of retinal neurites. Development *130*, 2479–2494.

McNew, J.A., Parlati, F., Fukuda, R., Johnston, R.J., Paz, K., Paumet, F., Söllner, T.H., and Rothman, J.E. (2000). Compartmental specificity of cellular membrane fusion encoded in SNARE proteins. Nature *407*, 153–159.

Mendes, H.F., van der Spuy, J., Chapple, J.P., and Cheetham, M.E. (2005). Mechanisms of cell death in rhodopsin retinitis pigmentosa: implications for therapy. Trends Mol. Med. *11*, 177–185.

Nakajima, K., Hirose, H., Taniguchi, M., Kurashina, H., Arasaki, K., Nagahama, M., Tani, K., Yamamoto, A., and Tagaya, M. (2004). Involvement of BNIP1 in apoptosis and endoplasmic reticulum membrane fusion. EMBO J. *23*, 3216–3226.

Nishiwaki, Y., Komori, A., Sagara, H., Suzuki, E., Manabe, T., Hosoya, T., Nojima, Y., Wada, H., Tanaka, H., Okamoto, H., and Masai, I. (2008). Mutation of cGMP phosphodiesterase 6alpha'-subunit gene causes progressive degeneration of cone photoreceptors in zebrafish. Mech. Dev. *125*, 932–946.

Pacione, L.R., Szego, M.J., Ikeda, S., Nishina, P.M., and McInnes, R.R. (2003). Progress toward understanding the genetic and biochemical mechanisms of inherited photoreceptor degenerations. Annu. Rev. Neurosci. *26*, 657–700.

Peter, F., Wong, S.H., Subramaniam, V.N., Tang, B.L., and Hong, W. (1998). Alpha-SNAP but not gamma-SNAP is required for ER-Golgi transport after vesicle budding and the Rab1-requiring step but before the EGTA-sensitive step. J. Cell Sci. *111*, 2625–2633.

Poggi, L., Vitorino, M., Masai, I., and Harris, W.A. (2005). Influences on neural lineage and mode of division in the zebrafish retina in vivo. J. Cell Biol. *171*, 991–999.

Rothman, J.E. (1994). Mechanisms of intracellular protein transport. Nature *372*, 55–63.

Ryu, S.W., Choi, K., Yoon, J., Kim, S., and Choi, C. (2012). Endoplasmic reticulum-specific BH3-only protein BNIP1 induces mitochondrial fragmentation in a Bcl-2- and Drp1-dependent manner. J. Cell. Physiol. *227*, 3027–3035.

Söllner, T., Whiteheart, S.W., Brunner, M., Erdjument-Bromage, H., Geromanos, S., Tempst, P., and Rothman, J.E. (1993). SNAP receptors implicated in vesicle targeting and fusion. Nature *362*, 318–324.

Sung, C.H., Schneider, B.G., Agarwal, N., Papermaster, D.S., and Nathans, J. (1991). Functional heterogeneity of mutant rhodopsins responsible for autosomal dominant retinitis pigmentosa. Proc. Natl. Acad. Sci. USA *88*, 8840–8844.

Tait, S.W., and Green, D.R. (2010). Mitochondria and cell death: outer membrane permeabilization and beyond. Nat. Rev. Mol. Cell Biol. *11*, 621–632.

Tam, B.M., and Moritz, O.L. (2007). Dark rearing rescues P23H rhodopsin-induced retinal degeneration in a transgenic Xenopus laevis model of retinitis pigmentosa: a chromophore-dependent mechanism characterized by production of N-terminally truncated mutant rhodopsin. J. Neurosci. *27*, 9043–9053.

Tolar, L.A., and Pallanck, L. (1998). NSF function in neurotransmitter release involves rearrangement of the SNARE complex downstream of synaptic vesicle docking. J. Neurosci. *18*, 10250–10256.

Vihtelic, T.S., Doro, C.J., and Hyde, D.R. (1999). Cloning and characterization of six zebrafish photoreceptor opsin cDNAs and immunolocalization of their corresponding proteins. Vis. Neurosci. *16*, 571–585.

Wells, J., Wroblewski, J., Keen, J., Inglehearn, C., Jubb, C., Eckstein, A., Jay, M., Arden, G., Bhattacharya, S., Fitzke, F., et al. (1993). Mutations in the human retinal degeneration slow (RDS) gene can cause either retinitis pigmentosa or macular dystrophy. Nat. Genet. *3*, 213–218.

Westerfield, M. (1995). The Zebrafish Book (University of Oregon Press: Eugene, OR).

Westphal, D., Dewson, G., Czabotar, P.E., and Kluck, R.M. (2011). Molecular biology of Bax and Bak activation and action. Biochim. Biophys. Acta *1813*, 521–531.

Whiteheart, S.W., Griff, I.C., Brunner, M., Clary, D.O., Mayer, T., Buhrow, S.A., and Rothman, J.E. (1993). SNAP family of NSF attachment proteins includes a brain-specific isoform. Nature *362*, 353–355.

Wilson, D.W., Wilcox, C.A., Flynn, G.C., Chen, E., Kuang, W.J., Henzel, W.J., Block, M.R., Ullrich, A., and Rothman, J.E. (1989). A fusion protein required for vesicle-mediated transport in both mammalian cells and yeast. Nature *339*, 355–359.

Woods, I.G., Lyons, D.A., Voas, M.G., Pogoda, H.M., and Talbot, W.S. (2006). nsf is essential for organization of myelinated axons in zebrafish. Curr. Biol. *16*, 636–648.

Yasuda, M., and Chinnadurai, G. (2000). Functional identification of the apoptosis effector BH3 domain in cellular protein BNIP1. Oncogene *19*, 2363–2367.

Zhang, H., Heim, J., and Meyhack, B. (1999). Novel BNIP1 variants and their interaction with BCL2 family members. FEBS Lett. *448*, 23–27.